

## Effect of Bi-doped on structural, morphological, and electrical properties of $\text{Sb}_2\text{O}_3$ nanostructured thin films for solar cells applications

Mustafa K. Hussien<sup>1\*</sup>, Ziad T. Khodair<sup>2</sup>, Asaad A. Kamil<sup>3</sup>, Sabah A. Salman<sup>4</sup>

<sup>1,2,3,4</sup>Department of Physics, College of Science, University of Diyala, Diyala, Iraq; jkoko4588@gmail.com (M.K.H.)

ziad\_tariq70@yahoo.com (Z.T.K.) asaad181162@yahoo.com (A.A.K.) pro.dr\_sabahanwer@yahoo.com (S.A.S.)

**Abstract:** Undoped and Bi-doped  $\text{Sb}_2\text{O}_3$  nanostructured thin films (3%, 5%, 7%, 9%) were prepared by chemical spray pyrolysis on glass substrates at 350°C. XRD confirmed polycrystalline cubic structure with (111) orientation, while FE-SEM revealed doping effects on surface morphology. Investigation revealed that film surfaces had a cubic-like nanostructure. The results of the electrical properties showed that, depending on the Hall effect, that p-type nature of all thin films. Solar cells with the composition ( $\text{Sb}_2\text{O}_3/\text{n-Si}$ ), which contains a layer of  $\text{Sb}_2\text{O}_3$  undoped and doped with Bi at a ratio of 9%, were prepared and investigated in dark and lighting conditions at room temperature for the heterojunction. The obtained results demonstrated that the value of the reverse current of the heterojunction (doped and undoped-  $\text{Sb}_2\text{O}_3/\text{n-Si}$ ) under illumination at a specific voltage is higher than that in the dark. This study aims to synthesis undoped  $\text{Sb}_2\text{O}_3$  films and doped with bismuth (Bi) at different ratios (3, 5, 7, and 9%) using the chemical spray pyrolysis technique and study structural, and electrical properties to get the optimum condition for fabricating solar cells and study its characteristics of the photovoltaic measurements (ISC, VOC, FF,  $\eta$ ).

**Keywords:** Bismuth, Doping, Solar cells structural and electrical properties, Thin films,  $\text{Sb}_2\text{O}_3$ .

### 1. Introduction

The growing population and the current speed of industrialization are causing increasing demand for energy. Day by day, energy deficit is being felt in many developing countries [1]. To overcome these energy-related problems, we have to develop advanced materials that are renewable, environmentally friendly, easily available, and suitable for cost-effective technology, high charge carrier mobility, non-toxic nature, low cost, chemical and thermal stability, and excellent electrical and optical properties. Similarly,  $\text{Sb}_2\text{O}_3$  is one of the early and most widely used inorganic semiconductors and candidate materials for the preparation of window layers in thin film solar cells [2]. However, doping with another ion is a successful technique applied by several groups in order to improve the optical properties and performance of semiconductor thin films [3].

Of all p-block elements, some significantly affect the material properties of  $\text{Sb}_2\text{O}_3$  films, and Bi is one of them. Several researchers reported on the structural, optical, and thermoelectric power properties of Bi-doped  $\text{Sb}_2\text{O}_3$  thin films prepared by the spray pyrolysis [4]. Still, it is necessary to study the influence of bi-doping on the electrical properties of the  $\text{Sb}_2\text{O}_3$  nanostructured thin film based on its concentration [5]. The parameters define the efficiency of solar cells in contrast to the morphological, optical, and thermoelectric power effects. Considering this, this study aims to investigate the influence of Bi dopant concentration on the structural, morphological, and electrical characteristics of  $\text{Sb}_2\text{O}_3$  nanostructured thin films. Subsequently, this work on bismuth-doped  $\text{Sb}_2\text{O}_3$  as a function of bismuth concentration could arouse the interest of a wide range of experts in the field for the development of new solar cell technologies.

Different techniques have deposited metal oxide thin films, including sol-gel, spray pyrolysis, atmospheric pressure chemical vapor deposition, pulsed laser deposition, green synthesis, co-deposition, and magnetron sputtering [6-10]. This study aims to synthesis undoped  $\text{Sb}_2\text{O}_3$  films and doped with bismuth (Bi) at different ratios (3, 5, 7, and 9%) using the chemical spray pyrolysis technique and study structural, and electrical properties to get the optimum condition for fabricating solar cells [11].

### 1.1. Background and Motivation

$\text{Sb}_2\text{O}_3$  is an n-type semiconductor commonly referred to as stibnite, with various fascinating properties. It has been employed in different kinds of optoelectronic devices, field emitters, gas sensors, and photocatalysts. Semiconductors in nanostructured form lead to a high surface-to-volume ratio, significantly enhancing the rate of reactions taking place at the surface, in addition to exhibiting extraordinary electronic characteristics like visible light sensitivity, quantum confinement, surface traps, and many more. Introducing the Bi dopant in host  $\text{Sb}_2\text{O}_3$  material leads to higher energy efficiency, making it an important photocatalyst and sensitizer for solar cells. Bi doping in semiconducting materials reduces the band gap, encouraging absorption of visible light. These properties implicate  $\text{Sb}_2\text{O}_3$  nano-films to be a prominent candidate for solar cells [12].

The energy conversion efficiency of the photoanode is fundamentally reliant on a few critical factors which include the electron lifetime, the cross-sectional area of the photoanode, and the diffusion length associated with the photoanode itself. These elements play essential roles in determining how effectively energy can be converted [13]. In addition to these primary factors, it is important to consider that the recombination of electron holes must be minimized to limit the possibility of negative carriers being introduced into the photoanode. This is pivotal for optimal performance. Both the electron lifetime and the diffusion length can be optimized by effectively reducing the electron-hole carrier recombination processes that take place inside the semiconductor material [14]. Numerous reports and studies have confirmed that Bi doping significantly enhances the performance of the semiconductor. Specifically, this research examines the Bi-doped properties of  $\text{Sb}_2\text{O}_3$ , noting several key aspects such as the effect of the Bi dopant, how the band gap variations manifest, the distinctive XRD patterns that are observed, and the DRS spectra which are ascertained to be directly related to the varying Bi content within the material. Consequently, the primary aim of this comprehensive study was the successful fabrication of  $\text{Sb}_2\text{O}_3$  nanostructure thin films that are doped with Bi, employing the spray pyrolysis technique as a viable method [15]. The given study is primarily directed towards enhancing solar cell efficiency for potential application in greenhouse settings. Solar modules, recognized as one of the most prevalent sources of renewable energy, have been attracting a considerable amount of attention in recent years. This is largely due to their numerous apparent advantages, such as eco-friendliness, sustainability, achieving energy independence, and significant reductions in economic expenditure, among other meaningful benefits they provide. Furthermore, these solar technologies contribute significantly to the reduction of greenhouse gas emissions and play a crucial role in the preservation of our precious natural resource [16].

### 1.2. Research Objectives

The research objectives are to evaluate the effect of bi-dosing on the structural, optical, and electrical properties of  $\text{Sb}_2\text{O}_3$  thin films that have been deposited on a glass substrate using the tape casting technique. The optimal bi doping concentration in the base precursor must first be obtained. Then, the effect of bi-dosing as a function of structural properties, such as the crystal structure and grain properties, should be investigated. The resulting modifications in the electrical and optical properties must also be explored in order to achieve the optimum sequence. The investigations must be continuous to explore the effect of such doping on the characteristics and applications of the two contact  $\text{Sb}_2\text{O}_3$  thin layered solar devices. The obtained results are expected to provide reliable correlations between structural changes and a variety of electrical performance metrics, which can act as obstacles or

driving forces for different solar cell properties. Based on the above, the synthesis method was chosen to possess such a structure and dispersible grains. The study of the properties was performed to confirm that the prepared films, from structural and dispersion points of view, apparently possess a significant change based on the prepared method.

In this work, the objectives are clearly defined. The evaluation of the structural, optical, and electrical properties of  $\text{Sb}_2\text{O}_3$  nanostructured thin films, for different optimal bi doses in the starting composition of the films, was chosen with an effective method for the development of  $\text{Sb}_2\text{O}_3$  optical window layers that should act as a hole-blocking layer, as well as a transition with the p-type silicon base with a conductive bi-doped nanostructured layer for Si and  $\text{Sb}_2\text{O}_3$  films deposited by the TCM technique that can form excellent building blocks in the development of such n-Si/nanometer metal oxide/ $\text{Sb}_2\text{O}_3$  nano-p-Si solar cells, with one of the next steps in design and exclusive optimization. A synthesis structural investigation of  $\text{Sb}_2\text{O}_3$  thin films is performed to determine the optimum starting composition of the  $\text{Sb}_2\text{O}_3$  precursors that will reveal a structural phase with granular nano-spherical-like structure with good adhesion properties among grains, within the tape-casted TCM process. The single-phase target must be present to examine the specific effect of bi-dose on the  $Q$ -factors of the secondary reflection of the granular  $\text{Sb}_2\text{O}_3$  film. Unwanted crystallographic signals in this study should be associated with the different charge states of antimony on the surface under different conditions, and these will never be linked to the film composition.

## 2. Experimental Section

The Bi-doped  $\text{Sb}_2\text{O}_3$  thin film samples have been synthesized using the chemical spray pyrolysis technique. Figure 1 presents a schematic of the chemical spray pyrolysis system that consists of multiple elementary components.

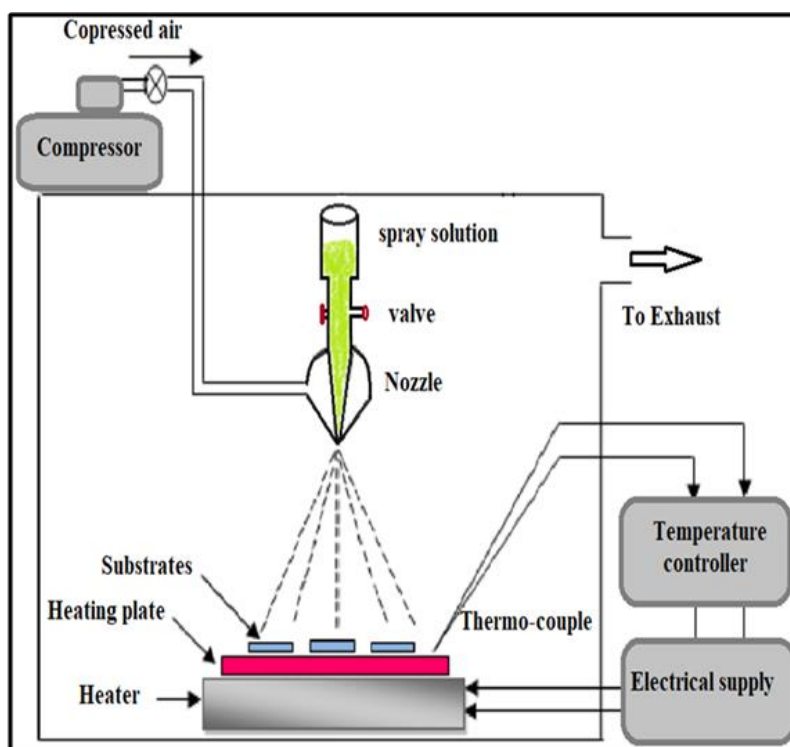


Figure 1.  
Chemical spray pyrolysis system.

The synthesized thin films deposited on carefully cleaned glass substrates with dimensions ( $2.5 \times 2.5 \times 0.1 \text{ cm}^2$ ). The  $\text{Sb}_2\text{O}_3$  thin films were fabricated utilizing antimony trichloride salt  $\text{SbCl}_3$  (228.11 g/mol) with a concentration of (0.02 M) in 100 ml of acetic acid solution. The solution stirred of (10 min) to obtain clear and homogeneous mixture as first solution. In the same procedure, the second solution prepared using hydrate bismuth nitrite salt  $\text{Bi}(\text{NO}_3)_3 \cdot 5\text{H}_2\text{O}$  (485.08 g/mol) as a dopant dissolved in 100 ml of distilled water with concentration of (0.02 M). The second solution added at different ratios of (3, 5, 7, and 9 %) to the first solution and then well mixed together using a magnetic stirrer for (30 min) to yield the optimal solubility of the solutions. The power source supplies electrical current to the heater and during (45 min.) the hot plate reached the desired temperature of ( $350 \pm 10 \text{ }^\circ\text{C}$ ). The cleaned glass substrates placed on the hot plate. The atomizer fixed vertically relative to the substrates with separation distance of (25 cm). Then, pour the prepared solutions into the atomizer cylindrical tube. By controlling the tap's valve to allow the solutions to flow into droplets, and then inject gas to replace the droplets with the desired spray. Spraying process continues for (10 sec) without interruption, followed by of (2 min.) pause to allow the substrates temperature to return to its initial values. This technique is iterated 13 times until it achieves the desired thin films thickness, as shown in figure 1. The substrates left on the hot plate of (30 min.) to promote the crystalline growth after completing the spraying procedure. Finally, switch off the electrical power supply and leave the substrates to cool down to room temperature.

### 3. Results and Discussion

#### 3.1. Structural Characteristics

##### 3.1.1. X-ray Diffraction (XRD)

Fig. 2 represents an X-ray pattern for antimony oxide ( $\text{Sb}_2\text{O}_3$ ) nanostructure thin films doped with bismuth (Bi) at different ratios (3%, 5%, 7%, and 9%) prepared by the chemical spray pyrolysis technique deposited on glass substrates at  $350 \text{ }^\circ\text{C}$ . The XRD pattern for  $\text{Sb}_2\text{O}_3$  thin films before doping was identified to be polycrystalline nature with cubic structure and include the (111), (222), (331), (440), (622), (444), and (662) diffraction peaks referred to ( $2\theta \sim 13.79^\circ, 27.76^\circ, 35.12^\circ, 46.09^\circ, 54.64^\circ, 57.26^\circ, 74.17^\circ$ ) respectively, which is agreement with ICSD card no. 01-072-1334 for  $\text{Sb}_2\text{O}_3$ . The preferred orientation along the peak intensity of (222) at ( $2\theta \sim 27.76$ ) decreased little with increasing doping at (3, 5, 7%) and then increased high at doping (9%), which means this sample has better crystal quality before doping. After doping, there was no clear effect on the peak locations, only a slight shift towards larger angle values and a clear increase in intensity when doping at (9%), which confirms that doping has led to improved crystallization, as well as the appearance of the plane (110) belonging to the compound  $\text{Sb}_2\text{O}_3$  at the angle ( $19.47^\circ$ ), which matches the values with ICDD card no. (00-011-0691).

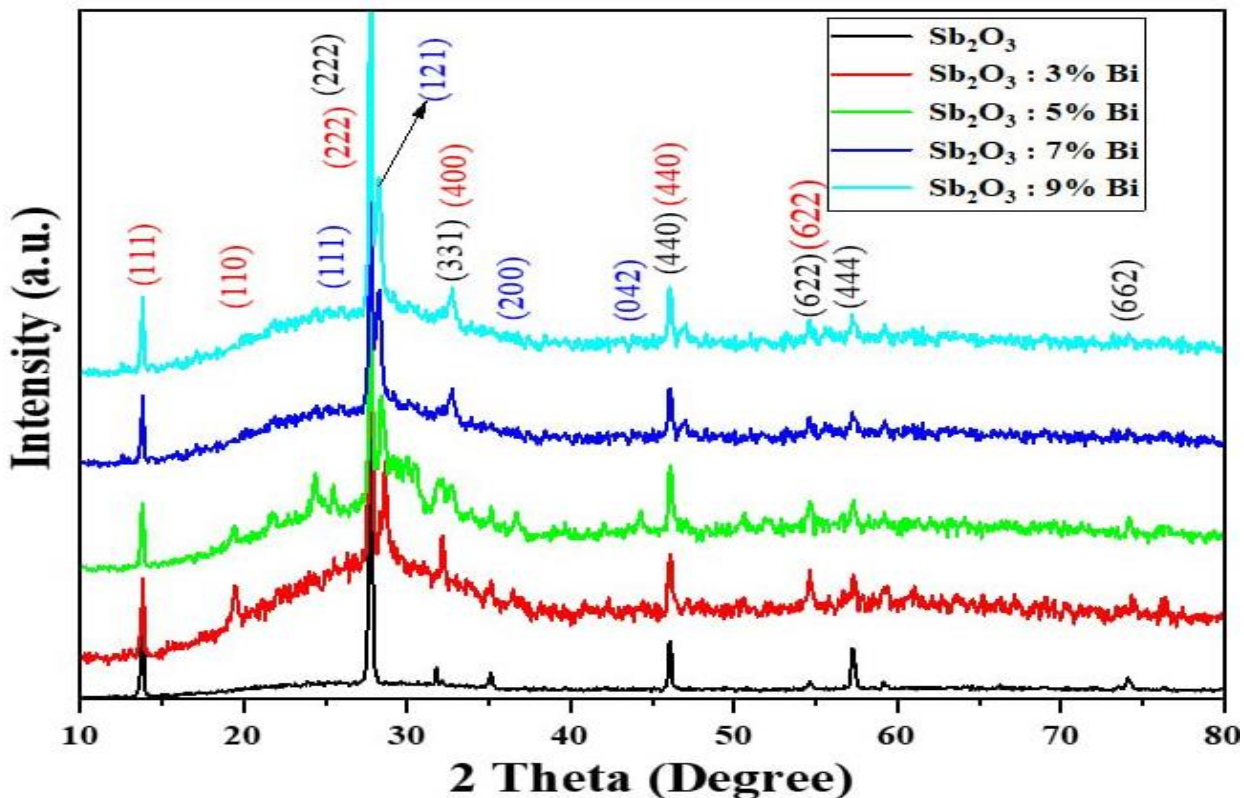


Figure 2. XRD patterns of synthesized samples (a) pure  $\text{Sb}_2\text{O}_3$  (b)  $\text{Sb}_2\text{O}_3$ : 3% Bi (c)  $\text{Sb}_2\text{O}_3$ : 5% Bi (d)  $\text{Sb}_2\text{O}_3$ : 7% Bi (e)  $\text{Sb}_2\text{O}_3$ : 9% Bi.

The crystallite size of pure  $\text{Sb}_2\text{O}_3$  and doped  $\text{Sb}_2\text{O}_3$  with Bi ions at different ratio (3, 5, 7 and 9 %) calculated based on the obtained highest XRD peaks using Debye Scherrer's formula [17-19].

$$D = \frac{K\lambda}{\beta \cos \theta}$$

where:

- D: average crystallite size (nm)
- K: shape factor, typically 0.94
- $\lambda$ : X-ray wavelength, given as 0.1506 nm in this case
- $\beta$ : full width at half maximum (FWHM) in radians
- $\theta$ : Bragg's angle (radians)

Table 2 shows the calculated crystallite size, FWHM, and d-spacing of synthesized samples, observing the slight reduction in the crystallite sizes of  $\text{Sb}_2\text{O}_3$  with the increasing of Bi ratio. We saw that the plane ( 222 ) crystallite size of undoped  $\text{Sb}_2\text{O}_3$  is 43.45 nm. The range of crystallite sizes for doped  $\text{Sb}_2\text{O}_3$  with Bi at different amounts (3, 5, 7, and 9%) was from 43.45 nm to 34.76 nm. These results show that the prepared samples have nanostructured thin films.

**Table 2.**  
Calculated XRD parameters of synthesized samples.

Samples	$2\theta$	FWHM (deg)	Crystallite Size (nm)	hkl	d- Spacing( Å)
Pure $\text{Sb}_2\text{O}_3$	27.757	0.1968	43.45	(222)	3.2138
$\text{Sb}_2\text{O}_3$ - 3% Bi	27.765	0.1968	43.45	(222)	3.2131
$\text{Sb}_2\text{O}_3$ - 5% Bi	27.257	0.1476	57.87	(222)	3.2140
$\text{Sb}_2\text{O}_3$ - 7% Bi	27.765	0.1476	57.93	(222)	3.2131
$\text{Sb}_2\text{O}_3$ - 9% Bi	27.759	0.2460	34.76	(222)	3.2137

### 3.2. Field Emission-Scanning Electron Microscopy (FE-SEM)

The surface morphology and microstructure features of the prepared films were investigated using FE-SEM device technology. This technology can magnify and accurately photograph material surfaces. The FE-SEM images of synthesized pure  $\text{Sb}_2\text{O}_3$  and doped with Bi at different ratios (3, 5, 7 and 9 %) presented in Figures 3 and 4 respectively, at different magnification of 3 kx and 200 kx . The  $\text{Sb}_2\text{O}_3$  thin films deposited by CSPT exhibit well-defined hexagonal-shaped cubic structures on their surfaces. High-magnification FE-SEM images reveal that the average dimensions are on the nanometer scale, indicating excellent grain growth. XRD analysis confirmed that the deposited materials have a hexagonal shape of nanoparticles with a cubic lattice [20] .

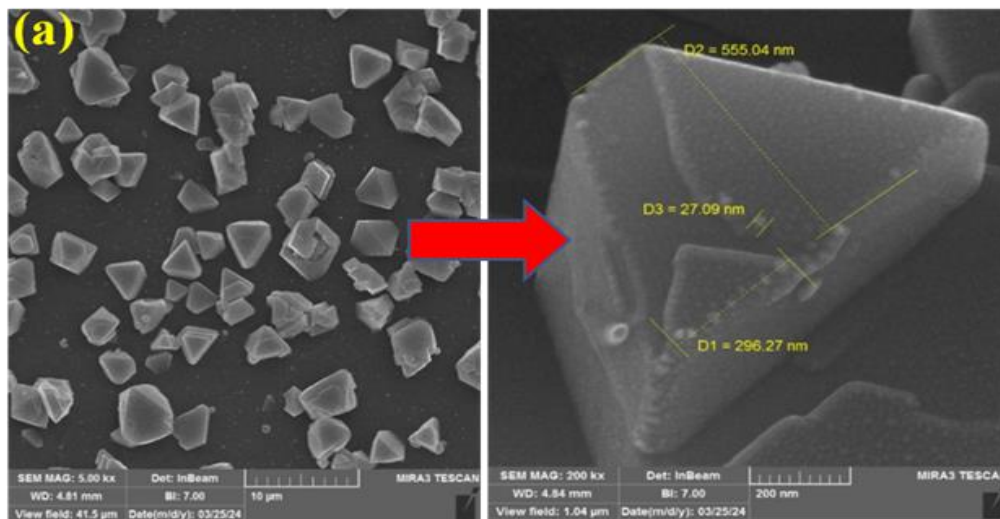


**Figure 3.**  
FE-SEM images of synthesized pure  $\text{Sb}_2\text{O}_3$

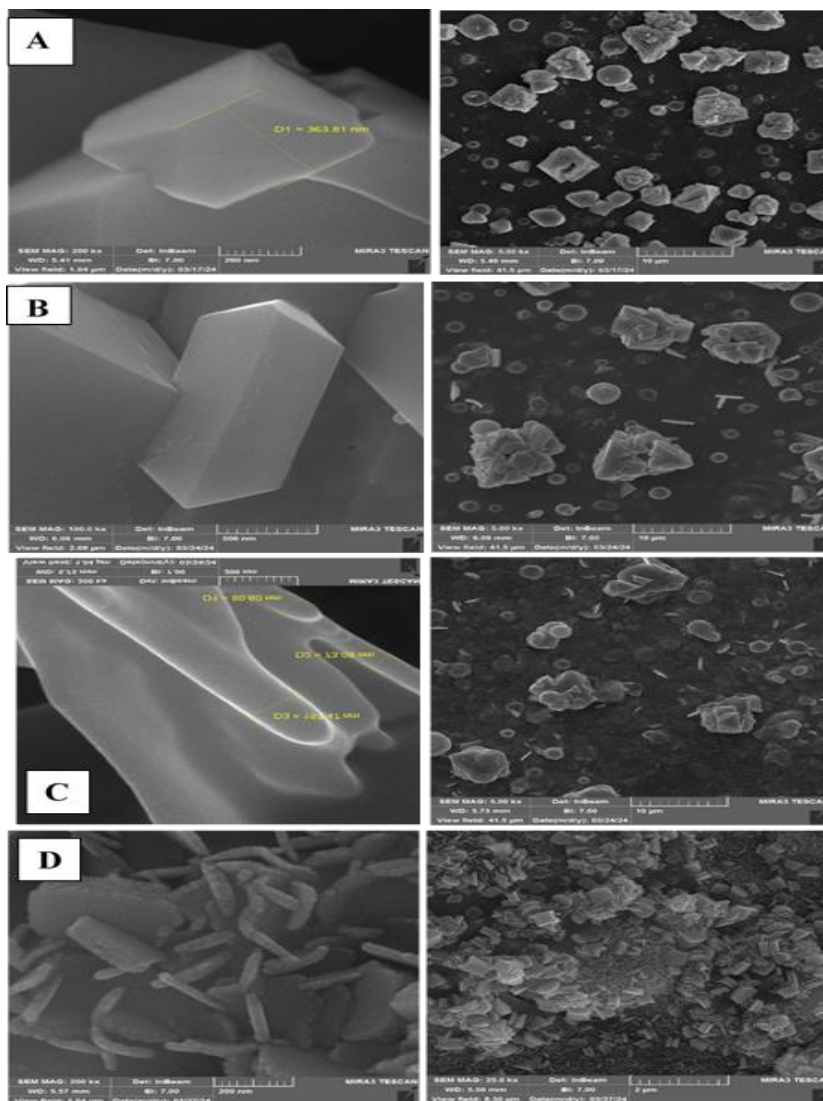


**Figure 4.** FE-SEM images of synthesized  $\text{Sb}_3\text{O}_2$  doped with Bi at different magnification (5 kx and 200 kx) (a)  $\text{Sb}_3\text{O}_2$ -3% Bi (b)  $\text{Sb}_3\text{O}_2$ -5% Bi (c)  $\text{Sb}_3\text{O}_2$ -7% Bi (d)  $\text{Sb}_3\text{O}_2$ -9% Bi.

### 3.3. Hall Effect

The Hall constant ( $R_H$ ), conductivity ( $\sigma$ ), electrical resistivity ( $\rho$ ), carrier concentration ( $n_H$ ), and mobility ( $\mu$ ) were calculated from the Hall potential, and the values obtained are listed in Table 5. In general, a negative sign of the Hall coefficient indicates an n-type conductive nature and a positive sign of the Hall coefficient indicates a p-type conductive nature. The thin films are composed of pure and doped antimony oxide ( $\text{Sb}_2\text{O}_3$ : Bi). Studies have shown that doping antimony oxide with different elements can change the Hall effect properties, by modifying the electronic structure of the material or the type of conductors, and can lead to an increase or decrease in the electrical conductivity of the material depending on the doping ratio and preparation conditions [21]. Antimony oxide films are usually semiconductors with negative charges (electrons) if the material is n-type, but in certain cases, p-type properties can be exhibited if impurities are present that lead to the presence of holes. When

antimony oxide films ( $\text{Sb}_2\text{O}_3$ ) are doped with impurities such as Bi or arsenic, the Hall effect can be changed, as doping affects the type and density of carriers (electrons or holes), and thus affects the photovoltaic and electrical properties of the material. Doping may increase the electrical conductivity or modify the type of carriers (n-type or p-type).

**Table 5.**

Hall effect of undoped and doped  $\text{Sb}_2\text{O}_3$ : Bi.

sample	$n$ ( $\text{cm}^{-3}$ )	$R_H$ ( $\text{cm}^3\text{C}^{-1}$ )	$\sigma$ ( $\Omega\text{cm}^{-1}$ )	$\mu$ ( $\text{cm}^2\text{V}^{-1}\text{s}^{-1}$ )	Type
$\text{Sb}_2\text{O}_3$	5.10E+16	1.22E+02	1.53E+01	1.88E+03	P
$\text{Sb}_2\text{O}_3$ :3%Bi	7.64E+16	8.17E+01	2.31E+01	1.89E+03	P
$\text{Sb}_2\text{O}_3$ :5%Bi	8.21E+16	7.60E+01	2.49E+01	1.89E+03	P
$\text{Sb}_2\text{O}_3$ :7%Bi	8.25E+16	7.56E+01	2.47E+01	1.87E+03	P
$\text{Sb}_2\text{O}_3$ :9%Bi	7.23E+16	8.64E+01	2.30E+01	1.99E+03	P

### 3.4. The Photoluminescence Spectrum Test (PL).

PL is a powerful tool for investigating the electronic properties of  $\text{Sb}_2\text{O}_3$  thin films. By investigation the photoluminescence spectrum, researchers can understand the details of the energy levels in the material and how electrons and holes interact with light, as well as the role of impurities and crystal defects. In many PL studies of  $\text{Sb}_2\text{O}_3$  films, it has been observed that the spectra exhibit behaviors that depend on film thickness, crystal structure, and the presence of impurities. For investigate, the intensity of the emitted light or the location of the peak in the spectrum can change with film thickness, reflecting the effects of nanoscale or growth defects. Illumination at specific wavelengths: The PL spectra of  $\text{Sb}_2\text{O}_3$  films often exhibit peaks or features at wavelengths between (350–600 nm). The main peak in PL: A peak can appear at (450–500 nm), which reflects transitions between energy levels in the material [22, 23]. Figure 5 presented the PL curves of pure  $\text{Sb}_2\text{O}_3$  and doped with different ratio of Bi element.

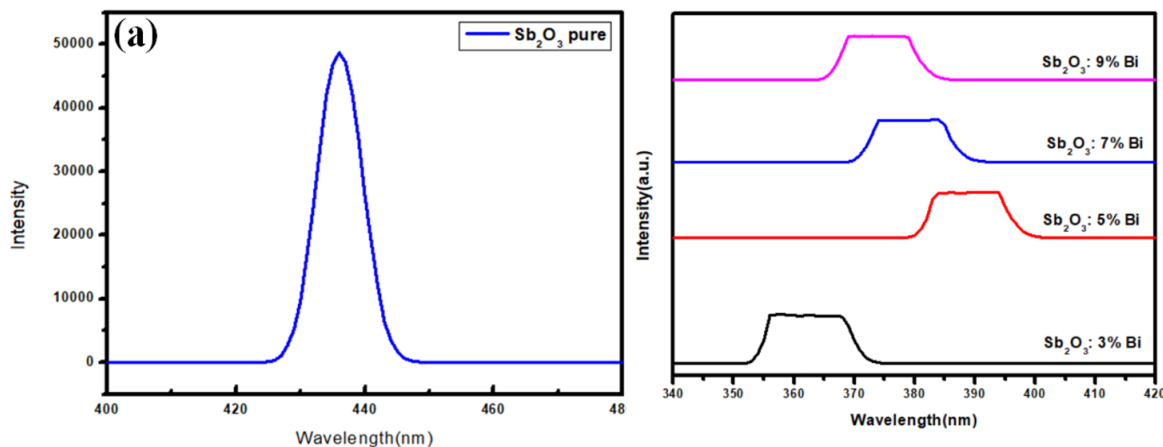


**Figure 5.**  
PL of (a) pure  $\text{Sb}_2\text{O}_3$  (b)  $\text{Sb}_2\text{O}_3$ :Bi at different ratio (3, 5, 7 and 9 %).

### 3.5. I-V Characteristic of thin Films

One of the most important applications of  $\text{Sb}_2\text{O}_3$  films as an active layer is solar cell devices. Two samples of films prepared from pure antimony oxide and doped with bismuth Bi at ratio of (9 %) were used to measure the parameters of solar cells. Figure 6 shows the current-voltage characteristics in dark conditions of the photo-detectors prepared in forward bias and reverse bias. The I-V results indicate that the fabricated heterojunction is asymmetric due to the difference in the current behavior in forward bias and reverse bias. The behavior is almost exponential in the forward-biased (asymmetric) case. In contrast, the behavior of the current in the reverse-biased case is almost linear and increases very



slightly with reverse bias [24, 25]. From the curves, in the case of forward bias, the current flowing through the heterojunction increases with the increase of the applied voltage. There are two types of current regions, the first region is known as the recombination current. The forward current of solar cells is very small at voltages below (0.004-0.012 ) [26]. We find that the bias voltage leads to a decrease in the rise of the barrier voltage because the applied voltage is opposite to the barrier voltage (V-VB) and the result of the multiplication of carriers, so the generation current occurs to reach a balanced state. In dark increase, the reverse current which refers to the dark current is independent of the bias voltage, i.e. it is very small, and this property is beneficial for the detector. The results indicated that the (I-V) characteristics of the detector do not show any breakdown in voltage up to approximately (5) volts, i.e. this region of the bias voltage are capable of saturation to operate the detector. It is not recommended to operate the photodetectors shown in Figure 15 at a voltage lower than (5) volts [27, 28].

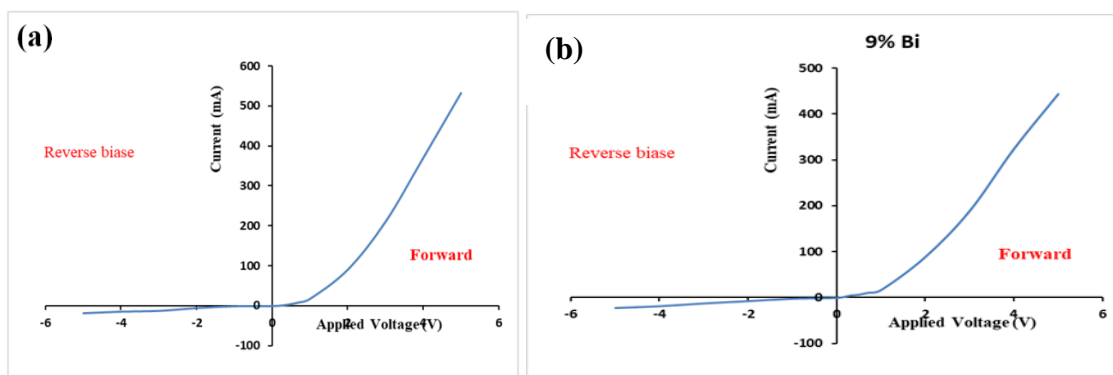


**Figure 6.** Current-voltage (I-V) characteristics curves of (a) pure  $\text{Sb}_2\text{O}_3$  (b)  $\text{Sb}_2\text{O}_3$  doped Bi (9 %) in dark conditions.

### 3.6. C-V Characteristics of (Undoped- $\text{Sb}_2\text{O}_3$ / n-Si/Ag) Junction Under Illumination

Most solar cells rely on their porous silicon composition, surface roughness, and the external configuration of the silicon crystal structure concerning the sample's thickness and layer count [22]. The photocurrent is the current generated by photon absorption and is regarded as a significant characteristic influencing spectral response. Figure 7 illustrates the (I-V) characteristics in both dark and illuminated conditions at room temperature for the heterojunction composed of ( $\text{Sb}_2\text{O}_3$ /n-Si/Ag). This structure incorporates a layer of undoped  $\text{Sb}_2\text{O}_3$ -Bi, doped with bismuth at a concentration of 9%, yielding a photocurrent when illuminated by a tungsten lamp at  $10 \text{ mWm}^{-2}$ . The figure indicates that photocurrent was detected solely under reverse bias conditions. It is evident that illumination results in a substantial enhancement of the reverse current. The photocurrent consistently aligns with the reverse bias direction, as it escalates with the widening of the depletion region. An increase in reverse bias voltage amplifies the internal electric field, thereby augmenting the likelihood of electron-hole pair separation. The figure clearly indicates that the optical current (photocurrent) rises with both the applied voltage and the intensity of the incident light, resulting in an increased number of charge carriers and an expanded depletion region with heightened reverse bias voltage, thereby enhancing the absorption and generation of electrons. The current value during illumination exceeds that in darkness, and in this scenario, the current is independent of voltage; rather, it is influenced by the photons incident on the heterojunction, resulting in enhanced mobility of charge carriers (electrons) and consequently an increase in current. It is clear from the figure that the value of the reverse current of the heterojunction (doped and undoped- $\text{Sb}_2\text{O}_3$ /n-Si /Ag) under illumination at a certain voltage is higher than that in the dark. As a result of the absorption of light, light leads to the generation of a photocurrent that contributes to the charge load as a result of the production of an electron-hole pair,

and this behavior results in useful information about the electron-hole pairs that are effectively produced by the photons falling on the junction.

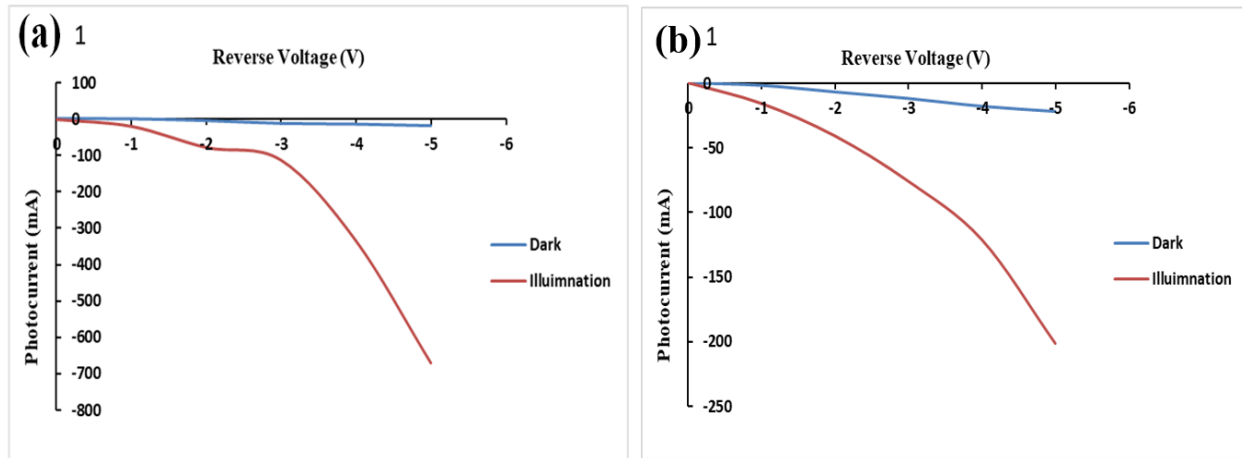


**Figure 7.** I-V characteristics in light and dark in the reverse bias state of the prepared cells (a) pure  $\text{Sb}_2\text{O}_3$  (b)  $\text{Sb}_2\text{O}_3$  doped Bi (9%).

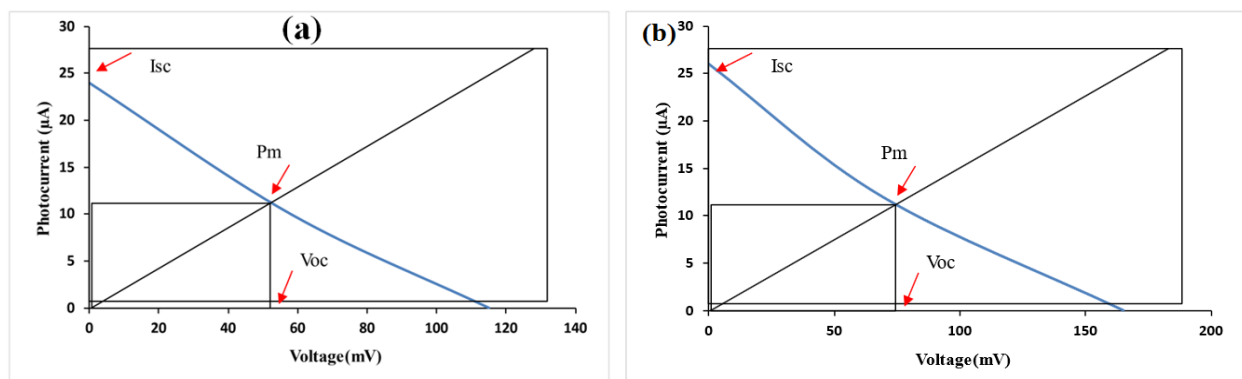
### 3.7. Efficiency of (P-N) Junction Solar Cells

Figure 8 shows the current-voltage (I-V) curves of the fabricated solar cells with  $\text{Sb}_2\text{O}_3/\text{n-Si}/\text{Ag}$  composition based on using pure  $\text{Sb}_2\text{O}_3$  and Bi-doped films as a (p) type absorber layer. Based on the current-voltage curve, the fill factor and efficiency of the solar cell were calculated as shown in Table 6. The obtained results revealed that the calculated parameters of the solar cells prepared were based on ( $\text{Sb}_2\text{O}_3$ ) films doped with bismuth (9%). In general, it is clear from the results that the solar cell with the composition  $\text{Sb}_2\text{O}_3:\text{Bi}/\text{n-Si}/\text{Ag}$  records the highest efficiency compared to the cell with the  $\text{Sb}_2\text{O}_3/\text{n-Si}/\text{Ag}$  composition. This is attributed to a decrease in structural defects and, as a result, an increase in mobility, which contributes to current transfer and increases the diffusion of carriers and thus increases the photocurrent.

**Table 6.**

Parameter values of solar cells prepared pure  $\text{Sb}_2\text{O}_3$  and doped Bi element thin films.

Samples	$V_{oc}$ (mV)	$I_{sc}$ ( $\mu\text{A}$ )	$V_m$ (mV)	$I_m$ ( $\mu\text{A}$ )	$\eta$ (%)	F.F (%)
pure $\text{Sb}_2\text{O}_3$	115	24	58	10	0.738853503	21.01449275
$\text{Sb}_2\text{O}_3$ : Bi (9%)	165	26	69	12	1.05477707	100.3636364



**Figure 8.** I-V curves of solar cells (a) pure  $\text{Sb}_2\text{O}_3$  (b)  $\text{Sb}_2\text{O}_3$  doped with Bi at a ratio of (9%).

#### 4. Conclusion

This work successfully synthesized the pure nanostructured  $\text{Sb}_2\text{O}_3$  thin films doped with different ratios of the Bi by the chemical spray pyrolysis method. The structural characteristics demonstrated that the thin films are nanostructures with a cubic structure type and growth in the same structure after doping with Bi, with hexagonal and tetrahedral particle shapes, showing excellent stoichiometry, and according to FE-SEM analysis, an investigation revealed that film surfaces had a cubic-like nanostructure. The electrical and optical characteristics revealed promising and attractive  $\text{Sb}_2\text{O}_3/\text{Bi}$  thin films to be applied in solar cells.

#### Transparency:

The authors confirm that the manuscript is an honest, accurate, and transparent account of the study; that no vital features of the study have been omitted; and that any discrepancies from the study as planned have been explained. This study followed all ethical practices during writing.

#### Copyright:

© 2025 by the authors. This open-access article is distributed under the terms and conditions of the Creative Commons Attribution (CC BY) license (<https://creativecommons.org/licenses/by/4.0/>).

#### References

- [1] D. P. Sapna, I. Sanjayan Sathasivam, P. Parkin, and Claire, "Highly conductive and transparent gallium doped zinc oxide thin films via chemical vapor deposition," *J. Carmalt, Sci. Rep.*, vol. 10, p. 638, 2020. <https://doi.org/10.1038/s41598-020-57789-x>
- [2] A. Narmada, P. Kathirvel, L. Mohan, S. Saravanakumar, R. Marnadu, and J. Chandrasekaran, "Jet nebuliser spray pyrolysed indium oxide and nickel doped indium oxide thin films for photodiode application," *Optik*, vol. 202, p. 163701, 2020. <https://doi.org/10.1016/j.ijleo.2019.163701>
- [3] B. Pandit, B. R. Sankapal, and P. M. Koinkar, "Novel chemical route for  $\text{CeO}_2/\text{MWCNTs}$  composite towards highly bendable solid-state supercapacitor device," *Scientific Reports*, vol. 9, no. 1, p. 5892, 2019. <https://doi.org/10.1038/s41598-019-42398-1>
- [4] N. Tigau, S. Condurache-Bota, R. Drasovean, J. Cringanu, and R. Gavrilă, "Vacuum annealing effect on the structural and optical properties of antimony trioxide thin films," *Rom. J. Phys.*, vol. 62, p. 604, 2017. <https://doi.org/10.1016/j.jphys.2017.02.001>
- [5] N. Tigau, V. Ciupina, G. Prodan, G. Rusu, and E. Vasile, "Structural characterization of polycrystalline  $\text{Sb}_2\text{O}_3$  thin films prepared by thermal vacuum evaporation technique," *Journal of Crystal Growth*, vol. 269, no. 2-4, pp. 392-400, 2004. <https://doi.org/10.1016/j.jcrysgro.2004.06.042>
- [6] H. A. Khalid and H. O. Noor, "Synthesis and characterization of hexagonal and tetrahedral monocrystalline  $\text{Sb}_2\text{O}_3$  thin films prepared by chemical spray pyrolysis technique," *IOP Conf. Series: J. Phys.*, vol. 1294, p. 022005, 2019.
- [7] N. Yesugade, C. Lokhande, and C. Bhosale, "Structural and optical properties of electrodeposited  $\text{Bi}_2\text{S}_3$ ,  $\text{Sb}_2\text{S}_3$  and  $\text{As}_2\text{S}_3$  thin films," *Thin Solid Films*, vol. 263, no. 2, pp. 145-149, 1995. [https://doi.org/10.1016/0040-6090\(95\)06757-X](https://doi.org/10.1016/0040-6090(95)06757-X)
- [8] I. El Zawawi, A. Abdel-Moez, F. Terra, and M. Mounir, "Substrate temperature effect on the optical and electrical properties of antimony trisulfide thin films," *Thin Solid Films*, vol. 324, no. 1-2, pp. 300-304, 1998. [https://doi.org/10.1016/S0040-6090\(98\)00783-X](https://doi.org/10.1016/S0040-6090(98)00783-X)
- [9] Y. R. Lazcano, L. Guerrero, O. G. Daza, M. Nair, and P. Nair, "Antimony chalcogenide thin films: Chemical bath deposition and formation of new materials by post deposition thermal processing," *Superficies y Vacío*, no. 9, pp. 100-103, 1999.
- [10] Z. A. Abed, A. H. Al Dulaimi, W. A. Shatti, A. N. Jasim, Z. T. Khodair, and S. Y. Khaleel, "Structural and optical characterization of nanostructured undoped  $\text{CuO}$  and cobalt-doped  $\text{CuO}$  thin films," *Journal of Ovonic Research Vol*, vol. 17, no. 6, pp. 581-587, 2021.
- [11] A. H. R. Al-Sarraf, Z. Khodair, M. I. Manssor, R. A. A. K. Abbas, and A. H. Shaban, "Preparation and characterization of  $\text{ZnO}$  nanotriangles and nanoflowers by atmospheric pressure chemical vapor deposition (APCVD) technique," in *In AIP Conference Proceedings (Vol. 1968, No. 1)*. AIP Publishing, 2018.
- [12] Z. T. Khodair, A. M. Mohammad, and A. A. Khadom, "Investigations of structural and magnetic properties of  $\text{Cu}_{1-x}\text{V}_x\text{O}$  nanostructures prepared by sol-gel method," *Chemical Data Collections*, vol. 25, p. 100315, 2020. <https://doi.org/10.1016/j.cdc.2020.100315>

- [13] A. M. Shano, A. A. Habeeb, Z. T. Khodair, and S. K. Adnan, "Effects of thickness on the structural and optical properties of Mn<sub>3</sub>O<sub>4</sub> nanostructure thin films," presented at the In Journal of Physics: Conference Series (Vol. 1818, No. 1, p. 012049). IOP Publishing., 2021.
- [14] S. A. Hameed, M. M. Kareem, Z. T. Khodair, and I. M. M. Saeed, "The influence of deposition temperatures on the structural and optical properties for NiO nanostructured thin films prepared via spray pyrolysis technique," *Chemical Data Collections*, vol. 33, p. 100677, 2021. <https://doi.org/10.1016/j.cdc.2021.100677>
- [15] Z. T. Khodair, B. A. Ibrahim, and M. K. Hassan, "Investigation on the structural and optical properties of copper doped NiO nanostructures thin films," *Materials Today: Proceedings*, vol. 20, pp. 560-565, 2020. <https://doi.org/10.1016/j.matpr.2019.12.018>
- [16] W. Shatti, Z. M. A. Abbas, and Z. Khodair, "Co-precipitation method for the preparation of Mn-Zn Ferrite and study their Structural and Magnetic properties," *JJ. Ovonic Res.*, vol. 18, pp. 473-479, 2022.
- [17] M. Kareem, Z. Khodair, and F. Mohammed, "Effect of annealing temperature on Structural, morphological and optical properties of ZnO nanorod thin films prepared by hydrothermal method," *Journal of Ovonic Research*, vol. 16, no. 1, pp. 53-61, 2020.
- [18] A. Saleh, N. BKER, and Z. T. Khodair, "effect of oxygen flow rate on structural and optical properties of sno 2 thin films prepared by apcvd technique," *Digest Journal of Nanomaterials & Biostructures*, vol. 13, no. 3, 2018.
- [19] Z. M. Abbas, W. A. Shatti, A. M. Mohammad, and Z. T. Khodair, "Magnetic iron oxide: Preparation and characterization for antibacterial activity applications," *Journal of Sol-Gel Science and Technology*, vol. 109, no. 2, pp. 534-542, 2024. <https://doi.org/10.1007/s10971-023-05876-4>
- [20] Y. Shinde, P. Sonone, and A. Ubale, "Synthesis and characterization of hexagonal and tetrahedral nanocrystalline Sb<sub>2</sub>O<sub>3</sub> thin films prepared by chemical spray pyrolysis technique," *Journal of Alloys and Compounds*, vol. 831, p. 154777, 2020. <https://doi.org/10.1088/1742-6596/1294/2/022005>
- [21] N. Tigau, V. Ciupina, G. Prodan, G. Rusu, C. Gheorghies, and E. Vasile, "Structure and optical properties of thermally vacuum evaporated Sb~ 2O~ 3 thin films," *Journal of Optoelectronics and Advanced Materials*, vol. 6, pp. 449-458, 2004.
- [22] T. Cebriano, M. Bianchi, and P. Javier, "Study of luminescence and optical resonances in Sb 2O3 micro-and nanotriangles," *Journal of Nanoparticle Research*, vol. 14, pp. 1-8, 2012.
- [23] A. Babar, S. Shinde, A. Moholkar, C. Bhosale, J. Kim, and K. Rajpure, "Structural and optoelectronic properties of antimony incorporated tin oxide thin films," *Journal of Alloys and Compounds*, vol. 505, no. 2, pp. 416-422, 2010. <https://doi.org/10.1016/j.jallcom.2010.07.037>
- [24] F. Ferrieu, A. Halimaoui, and D. Bensahel, "Optical characterisation of porous silicon layers by spectrometric ellipsometry in the 1.5–5 eV range," *Solid State Communications*, vol. 84, no. 3, pp. 293-296, 1992. [https://doi.org/10.1016/0038-1098\(92\)90023-5](https://doi.org/10.1016/0038-1098(92)90023-5)
- [25] B. Bensahel, L. T. Canham, and S. Ossicini, *Optical properties of low dimensional silicon structures*. Springer Science & Business Media, 2012.
- [26] L. Zuo *et al.*, "Sb<sub>2</sub>O<sub>3</sub> anode buffer induced morphology improvement in small molecule organic solar cells," *Applied Physics Letters*, vol. 99, no. 18, 2011. <https://doi.org/10.1063/1.3652874>
- [27] M. A. Green, "Solar cells: operating principles, technology, and system applications," *Englewood Cliffs*, 1982.
- [28] K. K. Manga *et al.*, "High-performance broadband photodetector using solution-processible PbSe–TiO<sub>2</sub>–graphene hybrids," *Advanced Materials*, vol. 24, no. 13, p. 1697, 2012. <https://doi.org/10.1002/adma.201104623>